pISSN: 2321 – 9742

The Sapience

Advances in Physical Science Research

Investigations of Twist Grain Boundary Phases in Chiral Liquid Crystals

Manisha Chaudhry
Department of Physics, JSSATE, Noida, 201301, UP, India
dr_manisha@jssaten.ac.in

Abstract

By means of Differential Scanning Calorimetry and high resolution polarizing microscopy it is observed that the in the pure cholestric liquid crystal shows twist grain boundary phases. Thermodynamically investigation in heating cycle observed TGBA* phase but in cooling cycle optical investigation TGBA* phase with smectic phase at different scanning rate. In the heating cycle chiral liquid crystals shows mixed phases due the pitch.

Keywords: Differential Scanning Calorimetry, smectic phase, liquid crystals.

1. Introduction

Twist Grain Boundary is an inimitable phase in liquid crystal field. The Twist Grain Boundary (TGB) phases have been become aware of in binary mixtures of nematic and cholesteric liquid crystals. The features of these an isomorphism are perturbed and they are very few in nature. These phases are equilibrium distribution of topological defects.

The existence of TGB phases was first renowned theoretically predicted by de Genes in 1972. This new beautiful phases are the analogy between the nematic (N) to smectic A (SmA) transition in liquid crystals and the normal to superconductor transition in metals. TGB is totally temperature dependent phase. The transition between the cholestric (N*) and SmA phases would occur either directly or would proceed through an intermediate phase which is characterized by a twisted lattice of screw dislocations [2, 3].

On the theoretical front, Renn and Lubensky [4] predicted a specific model for the Twist Grain Boundary SmA (TGB_A) phase. Its structure consists of SmA slabs of constant thickness l_b stacked in a helical fashion along an axis x parallel to the smectic layers of thickness d. Adjacent slabs are continuously connected via a twist grain boundary made of parallel screw dislocation lines analogous to magnetic vortices. The nematic director n (or equivalently the smectic layer normal N) is rotated across each grain boundary by finite angle $\Delta = 2 \tan^{-1} (d/2l_d)$, where d is the smectic period and l_d is the distance between parallel dislocation lines.

Consequently, twist penetrates the smectic structure just as magnetic field penetrates the type II superconducting phase via the abrikosov flux lattice. In the vicinity of a cholesteric (N*) – SmA- chiral smectic C (SmC*) point (where the type II condition is expected to be met), RL also predicted the existence of two new additional TGB phases, namely TGB_C and TGB_{C*} in which the smectic slabs are respectively, Sm-C and Sm-C*. This peculiarity

between three different Abrikosov phases is found in only and only in liquid crystals and does not exist in superconductors.

Renn and Lubensky [4] showed that the nature of the TGB state depends on the value of the twist angle $\Delta=2\pi\alpha$. If α is irrational, no periodicity exists along the pitch axis x and the state is incommensurate; If on the other hand α is rational (say $\alpha = p/q$ with p, q mutually prime integers), the structure is commensurate and x is q-fold screw axis, if this screw axis is not crystallograpically allowed (i.e. if $q \neq 2, 3, 4$ or 6), the TGB state has quasicrystalline rather than periodic crystalline symmetry and is commensurate in the plane y-z perpendicular to the pitch axis.

As pointed out by Renn and Lubensky [4], X ray scattering is intense on a Bragg cylinder of x axis and radius $Q_o=2\pi/d$ with a Gaussian profile along Qx of characteristic width $\xi^{-1} = 2\pi / (\lambda_{c2}d)^{-½}$, where λ_{c2} is the cholesteric pitch at the N*-TGB_A transition. The TGB structure is then incommensurate. For the commensurate TGB phases with noncrystallographic q, the fundamental set of reciprocal vectors forms a ring of equally spaced Bragg spots in the plane (Q_y, Q_z), perpendicular to the pitch direction Q_x [4].

The TGB_C structure has a priori one more degree of freedom then TGB_A, namely, the orientation of the vector n x N. Renn described the TGB_C structure with the assumption that the layer normal N remains perpendicular to the pitch direction x. Three consequences follow in the limit where long range electrostatic interactions are neglected: (i) the lowest energy structure correspond to both n and N perpendicular to x; (ii) the spontaneous electric polarization Ps α n α N [5] lies along x (such a TGBc phase is ferroelectric); and (iii) the TGB_A and TGBc structure factors are qualitatively identical.

2. Experimental Details

Pure sample of Cholesteric Nonanoate (CN) was obtained from the New Jersey, USA: 1-800-Acros-1 and it was used without further any additional treatment.

For the different mesophases, the transition temperatures were strong-minded by using a Differential Scanning Calorimeter (DSC) of Mettler Toledo (Model DSC822^e with STAR^e software) at two scanning rates, 5.0 ^{o}C/min and 10.0 ^{o}C/min. DSC thermograms were located with an accuracy of ±0.2 ^{o}C whereas the temperature reproducibility of the measurements was better than $^{\pm}$0.1 ^{o}C.

The optical investigation of mesophases were recorded by a transmitted light polarizing microscope, OLYMPUS BX 51P, magnification 10X and Lynsis software for taking the picture, The digital camera of model DP 70 fitted with microscope was used to identify the textures of different mesophases under different anchoring condition. The cell thickness was 6μm, which was used for the textural investigation [6].

Dielectric measurements as a function of temperature were carried out during the cooling cycle by impedance analyzer HP 4194A and temperature controllers Julabo F-25 and hot plate Instec HCS 302.

3. Results and Discussions

3.1 Thermodynamical Investigation

The DSC thermograms of CN at 5 ^{o}C/min and 10 ^{o}C/min scanning rate in heating cycle are shown in figs. 3.1 (a)-(c) respectively. The transition temperatures and enthalpies of CN are given in Table 3.1.

At 5 ^{o}C/min scanning rate the DSC thermograms of CN are displayed in fig. 3.1 (a)-(b). Fig 3.1 (a) shows two peaks in heating at 52.9 ^{o}C and 76.7 ^{o}C corresponding to K → TGBA* and TGBA* → N* transition and the enthalpies of K → TGBA* and TGBA* → N* transitions are 85.5 J/gm and 0.6 J/gm. The mass of sample was 5.6 mg. Fig. 3.1 (b) also shows two peaks in heating cycle centered at 77.8 ^{o}C and 91.8 ^{o}C temperature which correspond to K → TGBA*(N*) and (TGBA*) N*→ I transition. The enthalpies of the K → N* and N*→ I transitions are found as 87.8 J/gm and 2.0 J/gm respectively [7]. The mass of the sample was 2.2 mg for these studies.

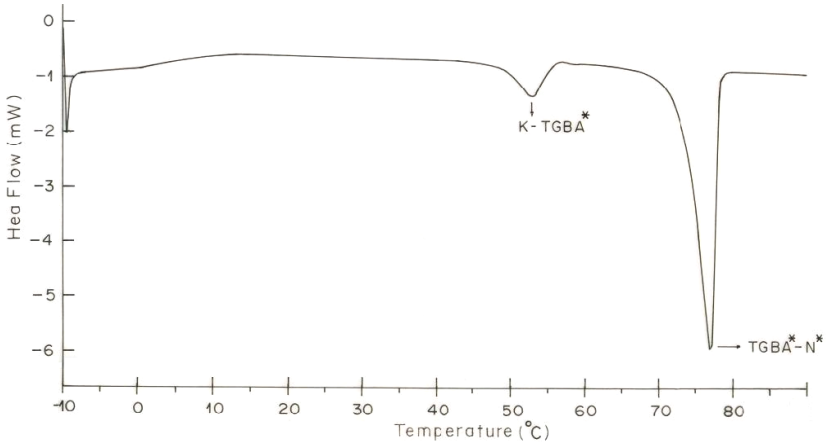

Fig. 1 (a): DSC thermogram of CN at 1 ^{o}C/min scanning rate.

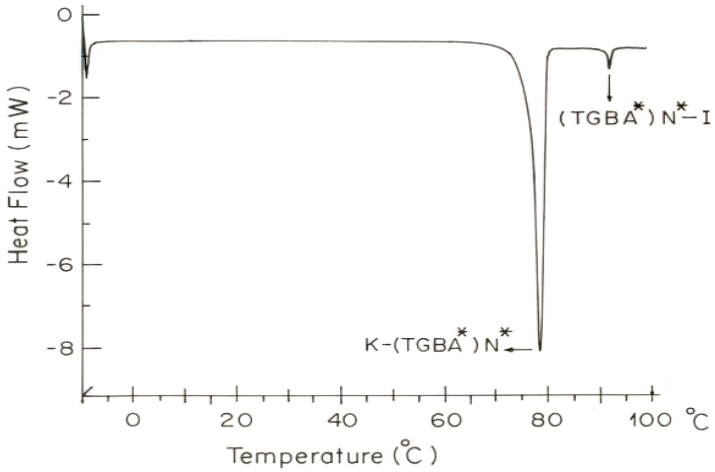

Fig. 1 (b): DSC thermogram of CN at 5 ^{o}C/min scanni

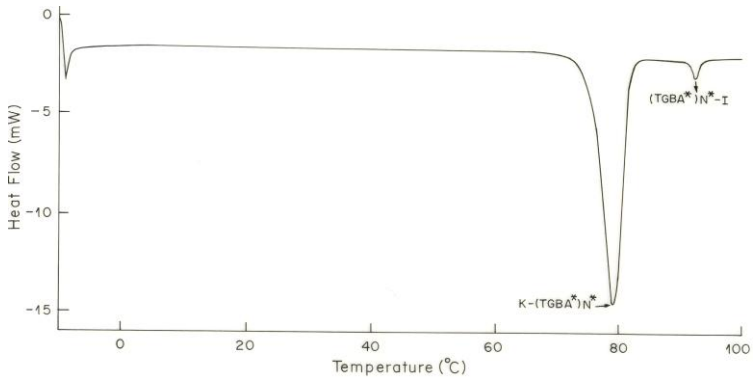

Fig. 1(c): DSC thermogram of CN at 10 ^{o}C/min scanning rate.

In heating cycle, at 10 ^{o}C/min scanning rate, the DSC thermogram of CN (fig. 3.1 (d)) shows two peaks at 78.3 ^{o}C and 92.2 ^{o}C temperature. First peak corresponds to K → (TGBA*) N* transition and second peak corresponds to (TGBA*) N* → I transition. First peak is broad; the shoulder on the right indicates presence of TGB phase. The enthalpies of these two transitions, K → N* and N* → I, are 55.6 J/gm and 1.1 J/gm respectively. Table 3.1 shows variation of transition temperature with respect to heating rate. It is found that transition temperatures increase linearly as the heating rate is increased .

We have recorded TGBA phase in pure CN for the very first time in thin unaligned film [7]. Earlier Nastishin et. al. [8] have shown existence of TGBA phase in CN by observing defect transformations at the N* - SmA transition in two geometries - suspended droplets with tangential anchoring conditions and free standing films. In some cases it has been very difficult to separate them, out of the background noise associated with the base line of the DSC thermograms but the associated optical texture have helped to locate them.[9-10]

3.2 Optical Investigation

The optical investigation is evidence for presence of TGB phases and it shown the very beautiful textures which is actually associated with different kinds of TGB structures. The transition temperatures recorded by polarizing microscopy observations and DSC differ from each other. It may be due to the fact that in microscopic observations the sample is not completely isolated from the surroundings. The optical textures of different TGB phases and other liquid crystalline phase have been recorded at different scanning rate 1 ^{o}C/min and 5 ^{o}C/min with the sample thickness of 6 μm.

When the molten CN is cooled, at 5 ^{o}C/min scanning rate, the separation of cholesteric phase (fig.3.2.a**)** from isotropic phase is marked at 92.2 ^{o}C by genesis of nucleations at several points which appear minute bubbles initially (spherullites), but which progressively grow radially.

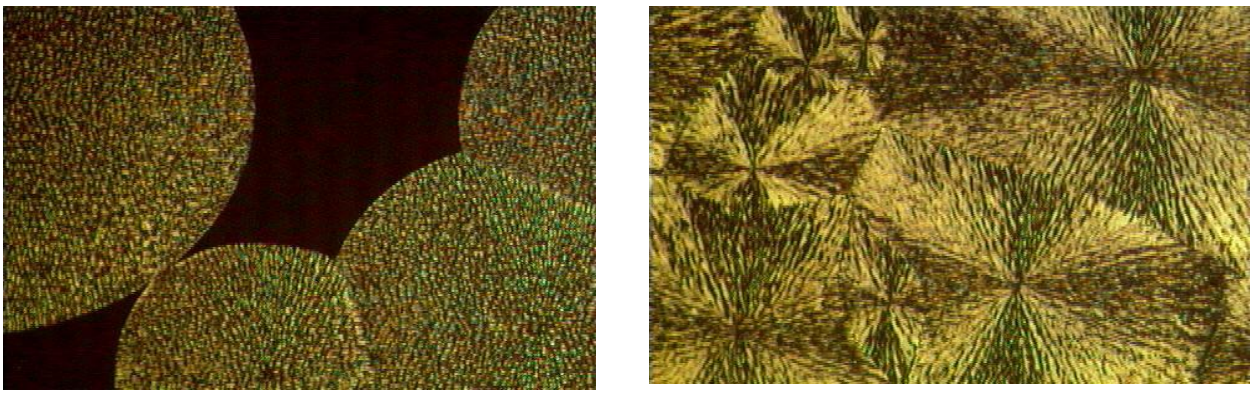

Fig. 2.a, b: Separation of N* phase from the molten sample of CN and Texture of TGBA* phase of CN

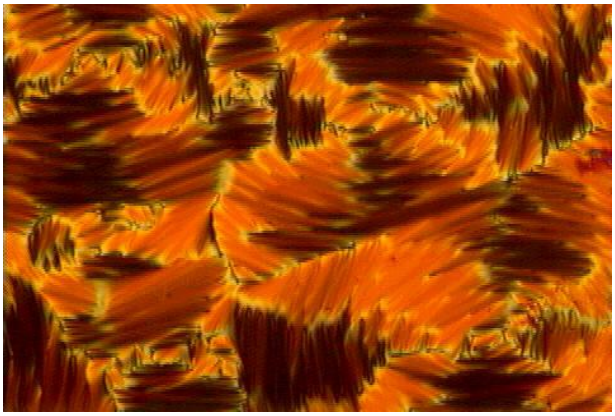
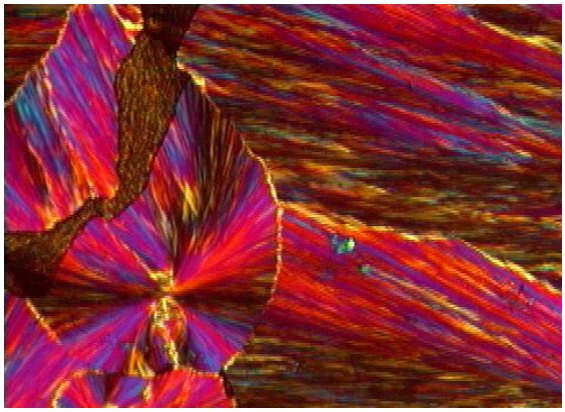

Fig. 2.c, d: Transformation of TGBA* to SmA focal conic type texture of CN and Crystal phase of CN

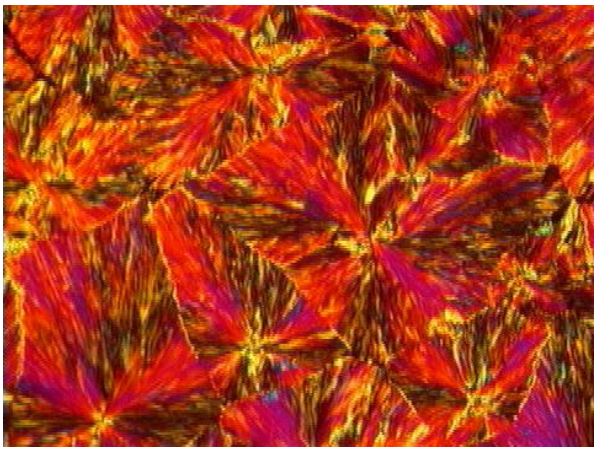
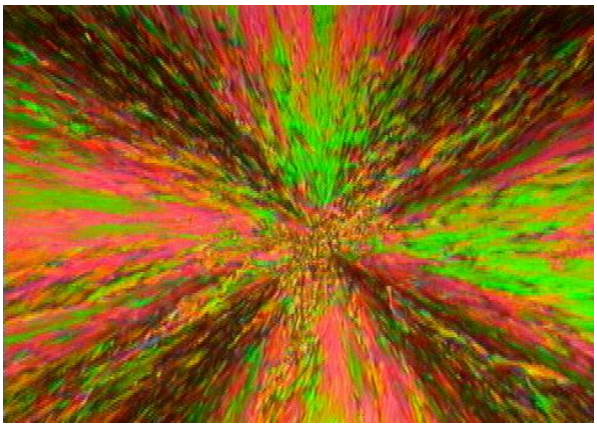

Fig. 2.e, f: Mixed crystal phase of CN, Filamentary texture of TGBA* phase of CN.

Initially it is transformed from N* $\rightarrow$ TGBA* with origin of black brushes from the centers of the spherulites finally (fig.3.2.b) it gives TGBA* cylindrical and cone like domain texture (CC type texture) with a χ - line at 79.5 ^{o}C. Fig.3.2.c shows TGBA* phase transforms to SmA phase giving focal conic texture at 77.8 ^{o}C, which ultimately crystallizes at 21 ^{o}C (fig.3.2.d).

In the heating run, at 10 ^{o}C/min scanning rate, the crystal phase (fig. 3.2.e) gives the mixed phases of CN 52.4 ^{o}C temperature (fig. 3.2.e). Such filamentary textures have been recorded earlier either in free standing films giving TGBA* phase [10] or in homeotropic samples [11].

The TGBA* strands get separated out as the temperature is increased and at 94 ^{o}C planar cholesteric texture is observed (fig. 3.2.f) which transforms to isotropic liquid crystal giving completely dark field of view.

A TGBA* is nothing else than an N* phase dressed with SmA layers at the microscopic scale much smaller than the wavelength of visible light. Thus the optics of TGBA* phase has no qualitative distinctive features compared to N* phase. A number of defects are topologically common to both TGBA* and N*.

A TGBA* phase is described by three directors, unit normal 'λ' common to all the layers, 'χ' a unit normal to a plane containing twist grain boundaries and $\tau = \lambda X \chi$. The three directors λ, χ and τ form a trihedron, that rotates by an angle 'ω' between steps of length l_b [12]. Difference between N* and TGBA* disclinations are physical not topological, i.e., they arise from the energy selection of distortions governed by the materialization of the χ

director and by the parallelism of smectic layers in the TGBA* phase. The defects occurring in non-planar preparations of smectic A are the focal conics. The smectic layers in the focal conic textures are supposed to be arranged in Dupin Cyclides and the most striking defects in this structure should be ellipses and hyperbolae in confocal relationship [12].

The polarizing microscopy observations at the N* $\rightarrow$ TGBA* transition show that same topological defects display easily recognizable features characteristic either of the N* or the TGBA* phase. In the N* phase, the field of the χ- director that emnates from the center of the spherulite has the geometry of a hedgehog point defect. The disclination lines of strength lines of strength k = 2, i.e., line defects which carry 4π rotations of the ortho normal frame of the directors about the line, escape into third dimension with no singularity remaining.
In the N* phase the χ- director is not materialized, there is no physical singularity attached to the χ-field. However in TGBA* the χ-singularities are materialized as singularities of the slabs.

In presented paper the CC textures form preferentially to the planar cholesteric textures (though exhibiting comparable elastic energies, if one takes double-twisting into account), essentially because they allow more possibilities, easier to adapt to uncontrolled anchoring conditions than the monocrytalline cholesteric textures [13]. The larger versatility of the CC configurations arises from the numerous undetermined parameters that they offer, as the shape, the size and the orientation of the domains. In particular, they have not really to be perpendicular to the cell plates though they look to be so under the microscope essentially because of the relatively thin cell thickness (a few μm) compared to their size (several hundred μm) [14].

4. Conclusions

In the presented paper CC textures form preferentially to the planar cholesteric textures (though exhibiting comparable elastic energies, if one takes double-twisting into account), essentially because they allow more possibilities, easier to adapt to uncontrolled anchoring conditions than the monocrytalline cholesteric textures. The larger versatility of the CC configurations arises from the numerous undetermined parameters that they offer, as the shape, the size and the orientation of the domains. In particular, they have not really to be perpendicular to the cell plates though they look to be so under the microscope essentially because of the relatively thin cell thickness (a few μm) compared to their size (several hundred μm).

5. Acknowledgment

I am thankful to Dr. A. M. Birader, Sci. G, National Physical Laboratory, New Delhi, for extending all facilities to pursue this work. I am sincerely grateful to Dr. K. K. Raina, Vice Chancellor of DTU, Dehradun for his encouragement.

6. References

1. P. G. de Gennes, Solid St. Commun.10, 753, (1972).
2. S. Fetter and P. Hohenberg. In superconductivity, edited by R. D. Parks (Dekker, New York, 1969).
3. D. Saint-James, G. Sarma and E. Thomas, Type ll Superconductors, (Oxford University Press, New York, 1969).
4. S. R. Renn, Phys. Rev. A 45, 953, (1992).
5. S. R. Renn, T.C. Lubensky, phys. Rev. A 38, 2132, (1988).

6. K.J. Ihn, J.A. Zasad Zinski, R. Pindak, A.J. Slaney, J.Goodby, Science 258, 275, (1992).

7. T.C. Lubensky, S. R. Renn, Phys. Rev.A 41,4392 (1990).

8. Nastishin, Yu. A., Kleman, M., Malthete, J. & Nguyen, H., T., (2001). Eur. Phys. J. E., 5, 353.

9. R. S. Pindak, Phys.Rev. Lett. 32, 43 (1974).

10. Goodby, J. W., Waugh, M. A., Stein, S. M., Chin, E., Pindak, R., and Patel, J. S., 1989, J. Am. Chem. Soc., 111, 8119.

11. Y. Galerne, Eur. Phys. J.E.3, 355 (2000).

12. Kleman, M., Nastishin, Yu. A. & Malthete, J., (2002). Eur. Phys. J. E., 8**,** 67.

13. I. Lelidis, et.al, Liquid Crystals, pages- 1437-1447, Issue-10, Vol.43, 2016.

14. Hale Ocak, Molecular Crystal and Liquid Crystals, pages- 7512-7515, Issue-1 vol 607, 2015.